NREL
NATIONAL RENEWABLE ENERGY LABORATORY

Electrical Characterization of Cu Composition Effects in CdS/CdTe Thin-Film Solar Cells with a ZnTe:Cu Back Contact

Preprint

Jian V. Li, Joel N. Duenow, Darius Kuciauskas, Ana Kanevce, Ramesh G. Dhere, Matthew R. Young, and Dean H. Levi

Presented at the 2012 IEEE Photovoltaic Specialists Conference
Austin, Texas
June 3–8, 2012

Conference Paper
NREL/CP-5200-54125
July 2012

Contract No. DE-AC36-08GO28308

NOTICE

Available electronically at http://www.osti.gov/bridge

Available for a processing fee to U.S. Department of Energy
and its contractors, in paper, from:

U.S. Department of Energy
Office of Scientific and Technical Information

P.O. Box 62
Oak Ridge, TN 37831-0062
phone: 865.576.8401
fax: 865.576.5728
email: mailto:reports@adonis.osti.gov

Available for sale to the public, in paper, from:

U.S. Department of Commerce
National Technical Information Service
5285 Port Royal Road
Springfield, VA 22161
phone: 800.553.6847
fax: 703.605.6900
email: orders@ntis.fedworld.gov
online ordering: http://www.ntis.gov/help/ordermethods.aspx

Cover Photos: (left to right) PIX 16416, PIX 17423, PIX 16560, PIX 17613, PIX 17436, PIX 17721

Printed on paper containing at least 50% wastepaper, including 10% post consumer waste.

Electrical Characterization of Cu Composition Effects in CdS/CdTe Thin-Film Solar Cells with a ZnTe:Cu Back Contact

Jian V. Li, Joel N. Duenow, Darius Kuciauskas, Ana Kanevce, Ramesh G. Dhere, Matthew R. Young, and Dean H. Levi

National Renewable Energy Laboratory, 15013 Denver West Parkway, Golden, Colorado 80401 USA

***Abstract* — We study the effects of Cu composition on the CdTe/ZnTe:Cu back contact and the bulk CdTe. For the back contact, its potential barrier (ϕ_{bc}) decreases with Cu concentration while its saturation current density (J_{0bc}) increases. For the bulk CdTe, the hole density (N) increases with Cu concentration. We identify a Cu-related deep level at ~0.55 eV whose concentration is significant when the Cu concentration is high. The device performance, which initially increases with Cu concentration then decreases, reflects the interplay between the positive influences (reducing ϕ_{bc} while increasing J_{0bc} and N) and negative influences (increasing deep levels in CdTe) of Cu.**

***Index Terms* — admittance measurement, capacitance-voltage characteristics, CdTe, charge carrier density, contacts, defect.**

I. Introduction

The effect of Cu is important to the operation of CdS/CdTe thin-film solar cells [1,2]. In this work, we study the effect of Cu on the back contact and CdTe absorber because they have a sensitive influence on open-circuit voltage (V_{oc}) and fill factor (FF) [3]. We vary the Cu composition in the ZnTe:Cu target used for the back contact in a series of CdS/CdTe devices and observe the consequent change in device performance. Secondary-ion mass spectroscmetry (SIMS) is used to quantify Cu composition near the back contact and in CdTe bulk. To study the effect of Cu on carrier transport, we use both electrical and optical techniques: temperature-dependent current-voltage (JVT), admittance spectroscopy (AS), capacitance-voltage (CV), drive-level capacitance profiling (DLCP), and time-resolved photoluminescence (TRPL). In the back contact, we find that the potential barrier decreases with Cu concentration whereas the saturation current density increases with Cu concentration. In the bulk CdTe, we find that the majority-carrier density increases with Cu concentration. At the same time, we identify a deep level due to Cu whose concentration is significant when the Cu concentration is high. The dependence of device performance on Cu composition can be understood by the interplay between these competing effects.

II. Experiment

All devices are superstrate type and have the same stack of layers: Corning 7059 glass, 400-nm SnO_2:F followed by 100-nm intrinsic SnO_2 by chemical vapor deposition at 550 ºC, 100-nm CdS by chemical-bath deposition at 92 ºC, 4–5-μm CdTe by close-space sublimation (CSS) at 620 ºC, 500-nm ZnTe:Cu by RF magnetron sputtering in 10 mTorr Ar at 300 ºC following $CdCl_2$ treatment (CSS in O_2/He, 400 ºC, 5min) and ion milling [1], 90-nm ITO by RF magnetron sputtering in 10 mTorr Ar at 300 K, and 50-nm Ni/ 3-μm Al metal grid by e-beam evaporation at 300 K. We used ZnTe:Cu targets with the following Cu weight percentage values: 0%, 0.3%, 1%, 2%, 4%, and 5%. We exclude the new 4% target in all characterizations except for the efficiency measurement because the 4% target was recently fabricated at a different time than the other targets.

We conducted JVT measurements with an HP 4140 semiconductor parameter analyzer and AC measurements (AS, CV, and DLCP) with an Agilent 4294A impedance analyzer. The AC modulation amplitude was varied from 0.015 to 0.215 Vp-p for DLCP, but kept constant at 0.055 Vp-p otherwise. The frequency was swept from 1 kHz to 1 MHz. The temperature range was 80–330 K. SIMS was performed using a Cameca IMS-5F instrument. Details of TRPL measurement are described in [4].

III. Device Performance and Composition Analysis

As shown in Fig. 1, the device efficiency first increases with Cu concentration and then decreases after reaching a peak at 2% Cu. The increasing trend from 0–2% Cu is contributed by V_{oc}, short-circuit current density (J_{sc}), and FF. The decreasing trend from 2–5% is contributed mostly by V_{oc} and FF.

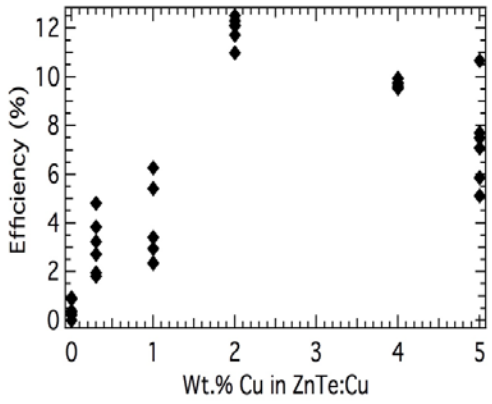

Fig. 1. Device efficiency of all devices in the series plotted against the Cu weight percentage in the ZnTe:Cu target.

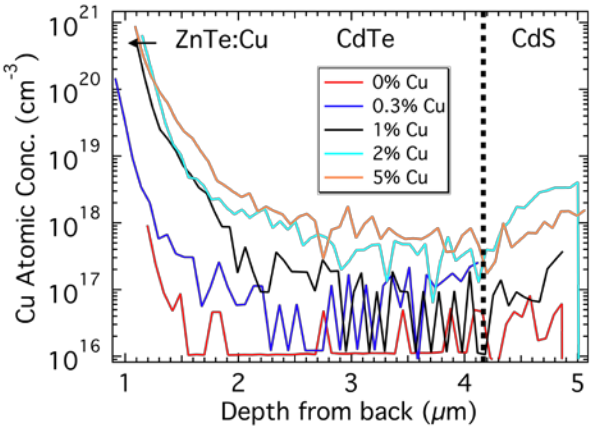

Fig. 2. SIMS depth profiles for samples with various Cu compositions.

The SIMS results in Fig. 2 confirm the expectation that devices fabricated with ZnTe:Cu targets of higher Cu weight percentage result in higher Cu concentration. This is indisputable near the back contact and in the CdTe bulk. As soon as the CdS layer is reached, however, the order is switched between 2% and 5% targets. Cu is expected to diffuse all the way into CdS, and the implication on device physics could be significant. We did not find the characterization results in this study particularly effective in revealing information on Cu in CdS. Therefore, we will focus on the effects of Cu near the back contact and in CdTe bulk. The motivation of this work is to understand how the device performance trends in Fig. 1 relate to the Cu composition trends in Fig. 2. To do that, we resort to results from a suite of electrical characterizations described below.

IV. Back-Contact Properties

Dark JVT data taken from a 5% Cu device under a mid-to-large forward bias are shown in Fig. 3. A rollover feature is clearly observed in Fig. 3 and is seen in all devices in this study. This rollover results from the double-diode behavior due to the back contact being non-ohmic [5]. Such a non-ohmic back contact is prevalent in CdTe devices because of the difficulty in doping CdTe and the relative deep location of the Fermi energy in CdTe compared to the work functions of most back-contact metals. Different physiochemical treatment and impurity incorporation have been investigated to mitigate the back-contact issue. The interest of this work is to find out how the Cu composition influences electrical properties of the back contact. Below, we show that useful parameters to characterize the back contact—namely, its potential barrier and saturation current density—can be extracted from a set of corroborative JVT-AS experiments.

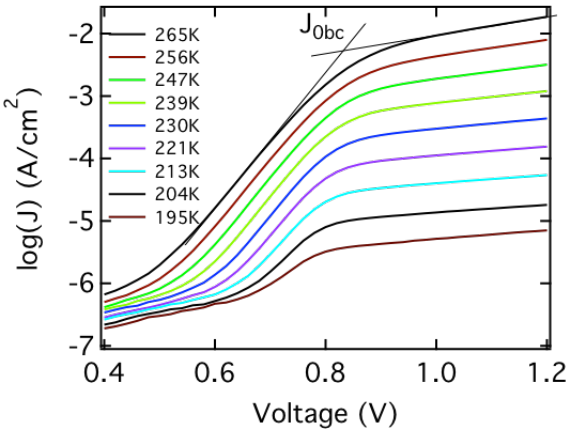

Fig. 3. JVT curves of device with 5% Cu showing rollover due to the back contact.

By constructing an Arrhenius plot of the onset current of rollover, which is determined from the intercept of the two slopes before and after the rollover (Fig. 3), the potential barrier and saturation current density can be extracted [5,6]. The back-contact potential barrier and saturation current density for all the devices are shown in Fig. 4. The potential barrier generally decreases with the Cu concentration. On the other hand, the saturation current density of the back contact increases with Cu concentration. Thus, Cu composition contributes positively to achieving an ideal back contact, i.e., one with a negligible potential barrier with infinite saturation current density. The double-diode circuit manifests itself not only in the DC characteristics, as described above, but also in the AC characteristics [5,6]. Next, we show that the back-contact potential barrier values extracted from dark JVT measurements are consistent with those extracted from admittance spectroscopy.

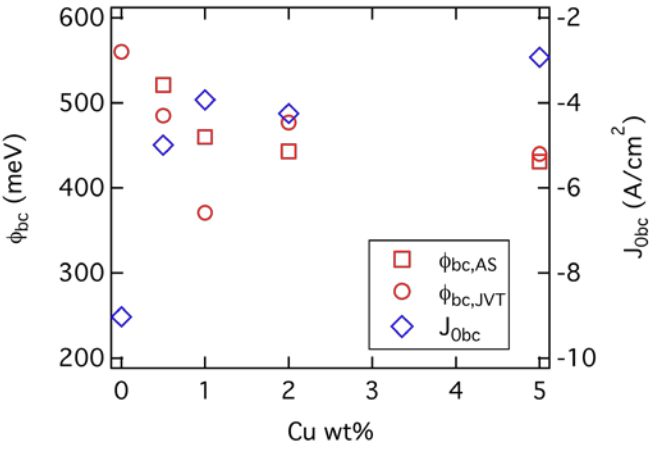

Fig. 4. The effect of Cu composition on the potential barrier (squares extracted from AS, circles extracted from JVT) and saturation current of the back contact (diamonds, extracted from JVT) at 300K (extrapolation may be needed if rollover occurs only at low temperatures). The errors in activation energy calculation are less than 20 meV.

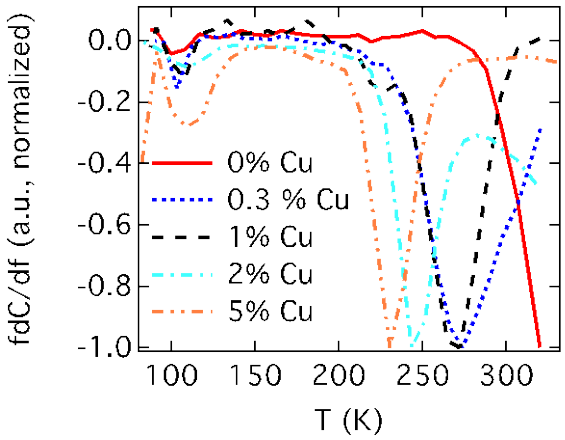

Fig. 5. The admittance spectroscopy data from all devices in the series, represented by the differential capacitance taken at 10 kHz. The negative peaks at higher temperatures (right) are due to the back-contact potential barrier. The negative peaks at lower temperatures (left) are due to majority-carrier freeze-out in the CdTe bulk.

In Fig. 5, we show the admittance spectroscopy data taken from all devices in the series at 0-V bias and 10-kHz frequency. There are a group of prominent negative peaks on the right (higher temperatures) and a group of less prominent peaks on the left (lower temperatures). As shown previously in a study [6] of back contacts with different treatments, the peaks on the right are signatures of the back contact. This signature has also been discussed in detail by Niemegeers et al. [7] and Eisenbarth et al. [8]. The peaks on the left are signatures of majority-carrier freeze-out in the CdTe absorber, which will be discussed in Section V. We note a rule of thumb for qualitative reading of data from thermally activated processes such as those shown in Fig. 5: the signatures at lower temperatures are of lower activation energy assuming everything else being equal. It is understood that the term "everything else" refers loosely to physical origin, device structure, and, more specifically, the pre-exponential factor of the thermally activated process. One observes in Fig. 5 that the negative peak progresses from right to left as Cu concentration increases. Applying the above rule of thumb, this progression qualitatively indicates that the activation energy associated with the negative peak decreases with Cu concentration. Indeed, this is quantitatively verified by activation energy data (squares) plotted in Fig. 4, which were extracted from Arrhenius plots constructed using the peak temperatures and corresponding frequencies such as shown in Fig. 5. Furthermore, the activation energies extracted from this particular signature of admittance spectroscopy closely agree with those from the dark JVT experiment. This agreement is in accordance with conclusions drawn from a previous study [6] and confirms that both activation energies are of the same physical origin, namely, the potential barrier of the back contact.

V. Bulk CdTe Properties

The capacitance-voltage measurement shown in Fig. 6 yields the apparent free-carrier density as a function of the depletion-region width in the CdTe absorber. In this work, the free carriers are presumably holes and the starting point of the depletion width is presumably at the CdS/CdTe interface. Evident in Fig. 6 is the strikingly consistent U-shape seen in the carrier density profile. As pointed out by a recent study [9], this U-shape is not only ubiquitous but also unique to CdTe devices because of the low doping in CdTe bulk, the relatively small thickness of the CdTe absorber, and the presence of a non-ohmic back contact. The low doping and finite thickness of CdTe bulk leads to full depletion of CdTe often at zero bias at room temperature assuming typical measurement frequency (10–100 kHz). If certain devices with higher doping or thickness happen to not be fully depleted at zero bias, they almost always quickly become fully depleted with modest addition of reverse bias. At this point of full depletion (or reach-through), CV is not measuring the carrier density in CdTe, but rather, that in the highly doped CdS or back contact. This is why the carrier density increases drastically when the depletion region width approaches the CdTe film thickness. The CdTe thickness of devices in this study is 4–5 μm, consistent with data in Fig. 6. The back contact also causes strong interference to the CV measurement. It has its own depletion width that could merge with that of the CdS/CdTe front junction to exacerbate the full-depletion problem at zero or reverse biases. Moreover, the back contact shares [9] DC and AC voltages with the CdS/CdTe front junction at forward biases. This causes the apparent carrier density to increase drastically under a forward bias, leading to the left branch of the U-shape in Fig. 6. As a result, reading carrier density from the zero-bias point is not the best practice. A more reliable practice is to read the

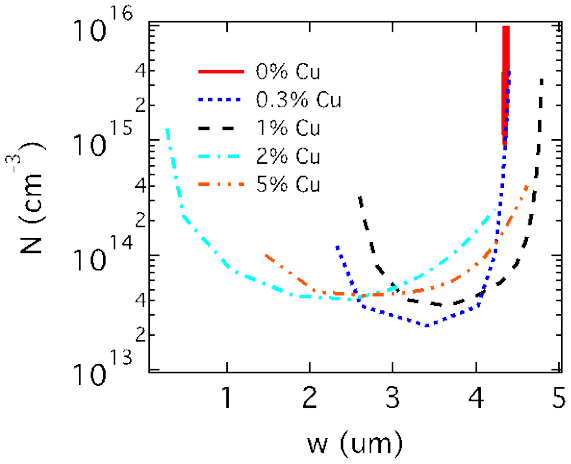

Fig. 6. Depth profiles of the apparent free hole density determined by capacitance-voltage technique from all devices in the series. The data were taken at a temperature of 300 K and a frequency of 100 kHz.

apparent free-carrier density value from the bottom of the typically U-shaped CV profile. A peculiar case is the 0% Cu device: ostensibly, it has the highest carrier density *and* the widest depletion width at zero bias. This contradicts expectation that higher carrier density results in *narrower* depletion width. In reality, this device has the lowest carrier density and therefore is fully depleted at zero bias or reverse biases, invalidating data taken at those biases. Data at forward biases are also not valid due to the device having the strongest rectifying back contact, as shown in Fig. 4. Discarding data from 0% Cu, the carrier density read from the bottom of the U-shape generally increases with Cu concentration and correlates well with V_{oc}. This trend is consistent with observations by other reports [2,10]. However, the quantitative correlation of carrier density with V_{oc}, as well as with Cu composition from SIMS data shown in Fig. 2, is poor. Per reasons described above, we attribute this to the limitations of the conventional CV technique and raise strong caution when it is applied to measurement of practical CdTe devices.

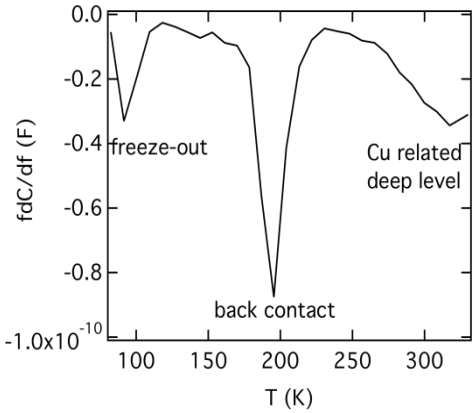

Fig. 7. Admittance spectroscopy data represented by the differential capacitance taken at 2 kHz reveals a Cu-related deep level in the device made from 5% Cu target.

We show in Fig. 7 the admittance spectroscopy data taken from a device made from the 5% Cu target. Data plotted in Fig. 7 were taken at a lower frequency (2 kHz) than those in Fig. 5 (10 kHz) to reveal the feature toward the high-temperature end of the measurement range. This signature has been associated [6] to a deep level due to Cu in the CdTe absorber. We saw this signature in all samples except the one made from the 0% Cu target. As shown in Fig. 8, the activation energy due to this level is 542 ± 12 meV. That is, this deep level is located at 542 meV above the valence band edge of CdTe. From a different device (2% Cu), a similar deep level of 598 ± 29 meV was extracted. Signal quality in other devices with 0.3% and 1% devices are not sufficient good to allow reliable extraction of an activation energy, although the same signature for the deep level are also observed near the maximum-temperature end of the measurement, as shown in Fig. 7. A deep level near mid gap, within 0.5–0.6 eV above the valence band edge of CdTe, has been observed in various studies [11-14] using both admittance spectroscopy and deep-level transient spectroscopy. In particular, the energy location of the deep level identified in this work and its correlation to Cu incorporation is similar to the H2 level reported by Balcioglu et al.[13].

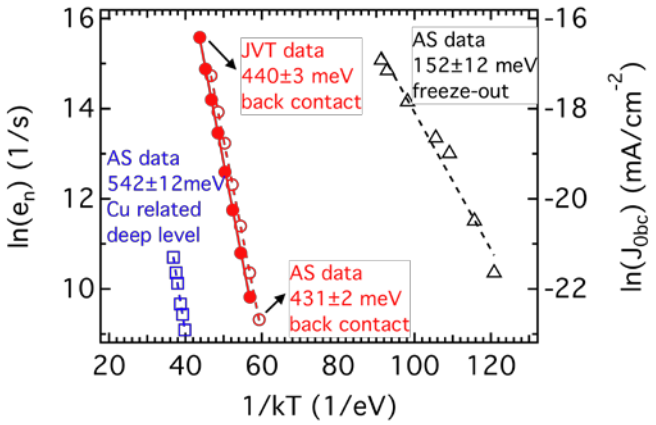

Fig. 8. Arrhenius plots constructed from AS data shown in Fig. 7 and JVT data shown in Fig. 3.

Comparison of the carrier density profiles by DLCP [15] and CV provides further information on the presence of the Cu-related deep level. Figure 9 shows that the carrier density extracted by CV is larger than that by DLCP between 2 and 3 μm depth in a device made from the 5% Cu target. The DLCP profile shows that the free-carrier profile is flat in this range. The increase of carrier density with reverse bias in the CV profile is due to electrostatic contribution from a significant concentration of the deep levels [9,15]. Such disagreement between CV and DLCP profiles is not seen in samples made from targets with less than 2% Cu, indicating that the concentration of defects is only significant for the higher Cu concentrations. The location of the Cu-related deep level being near mid-gap and its concentration being observable by DLCP signifies concern that it may play a detrimental role in bulk recombination, especially when the Cu concentration exceeds an optimal level.

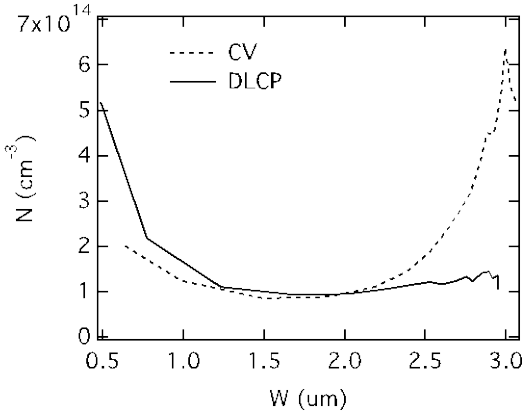

Fig. 9. CV and DLCP profiles taken at 2 kHz and 300 K. Data is from the device from the 5% Cu target.

We looked further for evidence in minority-carrier measurements at device level. However, minority-carrier lifetimes extracted from TRPL measurements did not indicate a clear decreasing or increasing trend with increasing Cu concentration. Presumably, the TRPL measurement is sensitive to the carrier-extraction phenomenon caused by the CdS/CdTe junction. More rigorous data analysis is currently under way to better extract the true carrier lifetime in CdTe bulk.

Minority-carrier diffusion length is a more relevant parameter to carrier collection efficiency because the carrier collection efficiency is ultimately determined (in part) by the minority-carrier diffusion length in the quasi-neutral CdTe absorber. Minority-carrier lifetime is only one of the two parameters [16] contributing to the minority-carrier diffusion length, the other being the minority-carrier mobility. At present, we do not have an effective method to extract the minority-carrier (i.e., electron) mobility. For lack of a better method, we measure the *majority*-carrier (i.e., hole) mobility and make the somewhat strong approximation that the ratio between the electron and hole mobilities is a constant. Information regarding the majority-carrier mobility is embedded [17,18] in the bias dependence of the freeze-out signature (Figs. 5, 7, and 8). To be more precise, this freeze-out is the *conductivity* freeze-out, instead of the *carrier-density* freeze-out. Using the method previously described [19,20], we extract hole mobility of 5.1 x 10^{-3}, 1.3 x 10^{-3}, and 5.6 x 10^{-3} $cm^2V^{-1}s^{-1}$ for devices made with ZnTe:Cu targets with 1%, 2%, and 5% Cu, respectively. Note that these values appear very low because they are measured at a low temperature of 100 K. At room temperatures, we typically measure values 2–3 orders of magnitude higher. The experimental error of these extractions probably exceeds 100%, considering that the extraction of carrier density (an input for extraction of mobility) is itself complicated and not accurate per our discussion on the subject of CV technique. Moreover, the presence of the non-ohmic back contact has not been taken into account in the current model. That probably contributed a large error to the extraction of mobility in the case of 1%, 2%, and 5% Cu, where the rectification characteristics of the back contacts are relatively weak (Fig. 4). In the case of 0% and 0.3% Cu, where the back contact is strongly rectifying (Fig. 4), the model described in references [19,20] is no longer applicable, which prevents one from obtaining meaningful extraction of hole mobility altogether. Within experimental error, it is not clear how much carrier mobility is sensitively influenced by Cu composition. Further methodological improvement is necessary to provide sufficient accuracy in mobility extraction for a clearer understanding of this subject. Considering our observation of the ~0.55-eV Cu-related deep level and its high concentration at high Cu concentration, we conjecture that minority-carrier lifetime is probably more sensitive to excessive Cu incorporation. Indeed, there have been reports [1,2] of reduced minority-carrier lifetime when Cu concentration exceeds a certain optimal level on very similar device structures. Although those reports used CdTe absorber and device structures quite similar to what is used in this study, they used different physical processes to tune the Cu incorporation.

VI. Conclusion

This study demonstrates that a comprehensive set of electrical characterizations are effective in investigating the electrically active defects due to Cu in the bulk CdTe, as well the dependence of back-contact properties on Cu composition. Corroborative JVT-AS experiments reveal the influence of Cu composition on the electrical properties of the back contact. The potential barrier there decreases with Cu concentration whereas the saturation current density increases with Cu concentration. Carrier density in the CdTe absorber extracted by CV profiling generally increases with Cu concentration. We provide analysis and evidence that the conventional CV technique needs to be used only with great caution on practical CdTe devices. AS experiment further shows the presence of a deep level due to Cu at ~0.55 eV above the valence band of the CdTe absorber. Comparison of carrier-density profiles extracted by CV and DLCP techniques reveals significant concentration of deep levels when the Cu concentration is greater than 2%. Combining the above characterization results, two types of effects can be attributed to increasing Cu concentration. The positive effect includes reducing the potential barrier of the back contact, increasing the saturation current density of the back contact, and increasing the free-carrier density in the CdTe absorber. The negative effect includes increasing deep levels due to Cu, hence causing more substantial recombination in CdTe bulk. Due to the interplay of these two opposing effects, the device performance first increases with Cu concentration and then decrease after reaching a peak at 2% Cu.

Acknowledgement

This work was supported by the U.S. Department of Energy under Contact No. DE-AC36-08GO28308 with the National Renewable Energy Laboratory.

References

[1] T.A. Gessert, W.K. Metzger, P. Dippo, S.E. Asher, R.G. Dhere, and M.R. Young, "Dependence of carrier lifetime on Cu-contacting temperature and ZnTe:Cu thickness in CdS/CdTe thin film solar cells," *Thin Solid Films*, vol. 517, pp. 2370–2373, 2009.

[2] S.H. Demtsu, D.S. Albin, J.R. Sites, W.K. Metzger, and A. Duda, "Cu-related recombination in CdS/CdTe solar cells," *Thin Solid Films*, vol. 516, pp. 2251–2254, 2008.

[3] J. Pan, M. Gloeckler, and J.R. Sites, "Hole current impedance and electron current enhancement by back-contact barriers in CdTe thin film solar cells," *Journal of Applied Physics*, vol. 100, pp. 124505 1–6, 2006.

[4] D. Kuciauskas, J.N. Duenow, A. Kanevce, J. V. Li, M.R. Young, and D.H. Levi, "Optical-fiber-based time resolved photoluminescence spectrometer for thin film absorber

characterization and analysis of TRPL data for CdS/CdTe interface," *Proceedings of 38th IEEE Photovoltaic Specialist Conference, Austin, Texas, June,* 2012.
[5] G. Stollwerck and J.R. Sites, "Analysis of CdTe back-contact barriers," *Proceedings of 13th European Photovoltaic Solar Energy Conference, Nice, France,* pp. 2020–2022, 1995.
[6] J.V. Li, S.W. Johnston, X. Li, D.S. Albin, T.A. Gessert, and D.H. Levi, "Discussion of some 'trap signatures' observed by admittance spectroscopy in CdTe thin-film solar cells," *Journal of Applied Physics*, vol. 108, pp. 064501 1–5, 2010.
[7] A. Niemegeers S. Gillis, and M. Burgelman, "Interpretation of capacitance spectra in the special case of novel thin film CdTe/CdS and CIGS/CdS solar cell device structures," *Proceedings of the 2nd World Conference on Photovoltaic Solar Energy Conversion, Ispra, Italy,* pp.1071–1074, 1998.
[8] T. Eisenbarth, T. Unold, R. Caballero, C.A. Kaufmann, and H.-W. Schock, "Interpretation of admittance, capacitance-voltage, and current-voltage signatures in Cu(In,Ga)Se_2 thin film solar cells," *Journal of Applied Physics*, vol. 107, pp. 034509 1–12, 2010.
[9] J.V. Li, A.F. Halverson, O.V. Sulima, S. Bansal, J.M. Burst, T.M. Barnes, T.A. Gessert, and D.H. Levi, "Theoretical analysis of effects of deep level, back contact, and absorber thickness on capacitance-voltage profiling of CdTe thin-film solar cells", *Solar Energy Materials and Solar Cells*, vol. 100, pp. 126–131, 2012.
[10] J. M. Burst, W.L. Rance, T.M. Barnes, M.O. Reese, J.V. Li, D. Kuciauskas, M.A. Steiner, T.A. Gessert, K. Zhang, C. Halmilton, K. Fuller, and C.A. Kosik Willams, "The effect of CdTe growth temperature and ZnTe:Cu contacting conditions on CdTe device performance," *Proceedings of 38th IEEE Photovoltaic Specialist Conference, Austin, Texas, June,* 2012.
[11] M.A. Lourenco, Y.K. Yew, K.P. Homewood, K. Durose, H. Richter, and D. Bonnet, "Deep level transient spectroscopy of CdS/CdTe thin film solar cells," *Journal of Applied Physics,* vol. 82, pp. 1423–1426, 1997.
[12] J. Versluys, P. Clauws, P. Nollet, S. Degrave, and M. Burgelman, "Characterization of deep defects in CdS/CdTe thin film solar cells by deep level transient spectroscopy," *Thin Solid Films*, vol. 451-452, pp. 434–438, 2004.
[13] Y.Y. Proskuryakov, K. Durose, B.M. Taele, G.P. Welch, and S. Oelting, "Admittance spectroscopy of CdTe/CdS solar cells subjected to varied nitric-phosphoric etching conditions," *Journal of Applied Physics,* vol. 101, pp. 014505, 2007.
[14] A. Balcioglu, R.K. Arhenkiel, and F. Hasoon, "Deep-level impurities in CdTe/CdS thin-film solar cells," *Journal of Applied Physics,* vol. 88, pp. 7175–7178, 2000.
[15] J.T. Heath, J.D. Cohen, and W.N. Shafarman, "Bulk and metastable defects in $CuIn_{1-x}Ga_xSe_2$ thin films using drive-level capacitance profiling," *Journal of Applied Physics,* vol. 95, pp. 1000–1010, 2004.
[16] S.M. Sze, *Physics of Semiconductor Devices*, John Wiley and Sons, New York, pp. 53, 1981.
[17] L.C. Isett, "Characterization of CdS/CdTe thin-film solar cells by admittance spectroscopy and deep-level transient spectroscopy," *Journal of Applied Physics,* vol. 82, pp. 3508–3517, 1984.
[18] D.V. Lang, J.D. Cohen, and J.P. Harbinson, "Measurement of density of gap states in hydrogenated amorphous silicon by space charge spectroscopy," *Physical Review B*, vol. 25, pp. 5285-5320, 1982.
[19] J.W. Lee, J.D. Cohen, and W.N. Shafarman, "The determination of carrier mobilities in CIGS photovoltaic devices using high-frequency admittance measurements," *Thin Solid Films*, vol. 480–481, pp. 336–340, 2005.
[20] J.V. Li, X. Li, D.S. Albin, and D.H. Levi, "A method to measure resistivity, mobility, and absorber thickness in thin-film solar cells with application to CdTe devices", *Solar Energy Materials and Solar Cells*, vol. 94, pp. 2073–2077, 2010.